Finite Dimension Thermodynamics for Optimizing Power Plants Including Heat Storage Device

Pierre Neveu, Baptiste Rebouillat, Quentin Falcoz

To cite this version:

Pierre Neveu, Baptiste Rebouillat, Quentin Falcoz. Finite Dimension Thermodynamics for Optimizing Power Plants Including Heat Storage Device. ECOS 2023 - THE 36TH INTERNATIONAL CONFERENCE ON EFFICIENCY, COST, OPTIMIZATION, SIMULATION AND ENVIRONMENTAL IMPACT OF ENERGY SYSTEMS, Jun 2023, LAS PALMAS DE GRAN CANARIA,, Spain. pp.136-147, ⟨10.52202/069564-0014⟩. ⟨hal-04311581⟩

HAL Id: hal-04311581

https://hal.science/hal-04311581v1

Submitted on 28 Nov 2023

HAL is a multi-disciplinary open access archive for the deposit and dissemination of scientific research documents, whether they are published or not. The documents may come from teaching and research institutions in France or abroad, or from public or private research centers.

L'archive ouverte pluridisciplinaire **HAL**, est destinée au dépôt et à la diffusion de documents scientifiques de niveau recherche, publiés ou non, émanant des établissements d'enseignement et de recherche français ou étrangers, des laboratoires publics ou privés.

Distributed under a Creative Commons CC BY-NC-SA 4.0 - Attribution - Non-commercial use - ShareAlike - International License

Finite Dimension Thermodynamics for optimizing power plants including heat storage device

Pierre Neveu[a], Baptiste Rebouillat[b], Quentin Falcoz[c]

[a] University of Perpignan Via Domitia,,Perpignan, France, pierre.neveu@univ-perp.fr
[b] PROMES-CNRS, Perpignan, France, baptiste.rebouillat@univ-perp.fr
[c] PROMES-CNRS, Odeillo, France, quentin.falcoz@promes.cnrs.fr

Abstract:

- This paper deals with the optimal integration of power plants including a storage device such as concentrated solar power plants. For such systems, numerous structures are possible, involving different number of heat exchangers, and for each of them, optimal operating temperatures to be found. Moreover, the heat storage system can be located at different temperature levels offering another degree of freedom when optimizing the whole system. If process simulators are nowadays very powerful tools for optimizing complex processes, they require to propose a primary design before any optimization steps. Finite-Dimension Thermodynamics (FDT) could help engineers to propose this primary design, close to the optimal one. To this aim, FDT method have been generalized for power generation systems including a storage device and any number of heat exchangers. An model of thermal storage system is also proposed which can be included in the FDT modelling. The optimization step consists in maximizing the power generation submitted to the thermodynamics constraints (first and second Laws) related to each heat exchangers, power block and thermal storage system. Remarkable results have been found: i) all the studied structures lead to the Curzon-Ahlborn efficiency when optimized, ii) for the same driving source (same temperature and same power), the output power production varies with N^{-2}, N being the number of the heat exchangers, iii) Charge and discharged times scenarios have a big impact on the optimal operating temperatures and on the resulting daily energy production.

Keywords:

Finite dimension thermodynamics, optimal integration, thermal storage, solar power plant.

1. Introduction

Finite-Time Thermodynamics aims to overpass the assumption of reversible, and consequently infinitely slow, transformations inherent to the Carnot cycle definition [1]. Chambadal [2] and Novikov [3] were the pioneers in 1957, proposing a power plant model that associates a reversible Carnot cycle driven by a heat source at high temperature T_H through an irreversible thermal resistance. These works were rediscover and completed by Curzon and Ahlborn [4] in 1975, who added a second thermal resistance coupling the reversible power block with the heat sink at low temperature T_L. All these previous studies were seeking the optimal temperatures between which the Carnot cycle must operate to ensure maximum power production. They demonstrated that at this maximum power point (MPP), the efficiency is equal to the so called 'nice radical efficiency' $\eta_{MPP} = 1 - \sqrt{T_L/T_H}$. De Vos [5] and Bejan [6] extended the Finite-Time Thermodynamics (FTT) to the Finite-Size or Finite-Dimension Thermodynamics (FDT) [7], [8]. The main difference is that the energy and entropy balances are here applied to the power plant itself, operating in a steady state, and not to the working fluid evolving in time over a cycle as done in FTT studies. Consequently, the method is no longer limited to Carnot engines, but can be applied for all types of engines. This leads to define endoreversible engine [5] for those internal entropy production is null or negligible. In that case, FTT and FDT lead to similar results, in particular to the nice radical efficiency at the MPP.

From these first studies, FTD/FDT methods have been successfully applied to a wide variety of systems such as refrigerators and heat pumps [9], distillation systems [10], chemical reactions [11] , wind power [12] or solar power [13]

However, the reliability of the results is often subjected to much criticism due to the assumptions underlying the FTT/FDT:

1. Linear driving force.
2. Endoreversible nature of the cycle.
3. Availability of powerful tools for industrial process optimization such as Aspen, Dymola or TRNSYS.

We obviously agree with these limitations. However, process simulators/optimisers require a mandatory first step: to propose a guessed design for initiating the optimisation process. This is the main objective of the FTT/FDT methodology: to define an initial design, deduced from thermodynamics, which could be used as a basis for further optimisation. Following this objective, the two first items seems reasonable: linear laws are commonly used in engineering pre-design, and endoreversible cycles are quite close to actual cycles as main irreversibility sources appear in the heat exchangers linking the process with the external heat sources . Moreover, Meunier et al. [14] and Castaing et al. [15] showed that an equivalent endoreversible cycle could be substituted to any sorption refrigeration irreversible cycles. This result also applies to any thermodynamics cycles. Conversely, passing from an endoreversible cycle to an actual cycle is also possible: in Reference [16], FDT method was used in order to find the optimal operating conditions of a endoreversible cycle, from which the optimal operating conditions of an actual Hirn cycle were deduced (i.e condensing and evaporating pressures and inlet turbine temperature). Nevertheless, FDT models are restricted to basic architectures of power plant: a single power cycle exchanging heat with two reservoirs through two heat exchangers (HX) whereas actual power plants often include more heat exchangers. PWR nuclear power plants use a primary heat transfer fluid (HTF), that induces two heat exchangers in the hot side: the reactor and the steam generator. In contrast, BWR use a single heat exchanger in the hot side: the reactor itself. The cooling loop can also involve one (condenser for direct through cooling) or two HXs (condenser and cooling tower for indirect cooling). A question then rises: does the HX number affect the optimal operating temperatures, the output power, and the efficiency of the cycle at the MPP? Similar issue appears for Concentrated Solar Power (CSP) plants, which can also involve one (Direct Steam Generator, DSG) or two (indirect heating) hot HXs. In addition, most of CSP plants include a thermal energy storage (TES) system, which adds complexity and diversity in possible architecture: the storage system can be direct (same fluid acts as HTF and storage medium) or indirect (two different HTFs flow in the solar loop and in the power block hot loop). Consequently, thermal storage device should be integrated in the FDT analysis. Therefore, the objectives of this work are twofold:

1. Extend the FDT methodology to processes that include a heat storage device.
2. Investigate the impact of TES and number of HX on the power plant optimal temperatures, power output and efficiency at the MMP.

In addition to these two original contributions, the optimization problem is solved without any assumption concerning the endoreversibility of the TES and the power block: the second law is treated here as an inequality while endoreversibility is usually assumed in FDT studies.

2. Problem definition

The FDT formalism requires to substitute a thermodynamic equivalent system to the real components involved in the power plant. The method is detailed in [16] and is briefly outlined here for heat exchangers and power blocks. An equivalent system is then proposed for TES systems. Finally, the optimisation problem is defined.

2.1. Equivalent heat exchanger and power block

Heat exchangers can be modelled by a thermal conductance K, transferring the heat flux $\dot{q}$ between two thermostats whose temperatures are equal to the mean entropic temperatures ($\tilde{T} = \Delta h/\Delta s$) of the cold and hot fluids. The heat flux can then be simply expressed by a Newton law:

$$\dot{q} = \mathrm{K}\left(\tilde{T}_H - \tilde{T}_L\right) \tag{1}$$

For power blocks, the same concept applies: any power cycle can be assessed through an equivalent cycle operating between two reservoirs à $\tilde{T}_H$ and $\tilde{T}_L$. For Rankine or Hirn cycles, these two temperatures are the entropic mean temperatures related to the working fluid when crossing respectively the steam generator and the condenser. First and Second Laws then write:

$$\dot{q}_H - \dot{q}_L = \dot{w} \tag{2}$$

$$\frac{\dot{q}_H}{\tilde{T}_H} - \frac{\dot{q}_L}{\tilde{T}_L} = -\dot{\sigma}_i \leq 0 \tag{3}$$

with $\dot{\sigma}_i$: internal entropy production (W/K)

$\dot{w}$: output power (W)

Notice that if $\dot{\sigma}_i$ = 0, Eqs. (2) and (3) define the endoreversible cycle.

2.2. Equivalent Thermal Energy Storage system

A two-tank heat storage device is considered (**Figure 1a**). Upstream, $\dot{m}^H$ flow enters the high temperature loop at temperature T_{out}^H, and returns to the TES system at higher temperature T_{in}^H. Downstream, $\dot{m}^M$ flow enters the medium temperature loop at T_{out}^M, and returns to the TES system at lower temperature T_{in}^M. The difference between the two mass flows is stored in or taken from either of the two tanks, hot at T^H. and cold

T^C. **Figure 1b** presents the operation scenario. Constant thermal powers are assumed here, but the method applies also for varying power. Hot loop operates during the duration t^H and the user demand is active during the duration t^M.

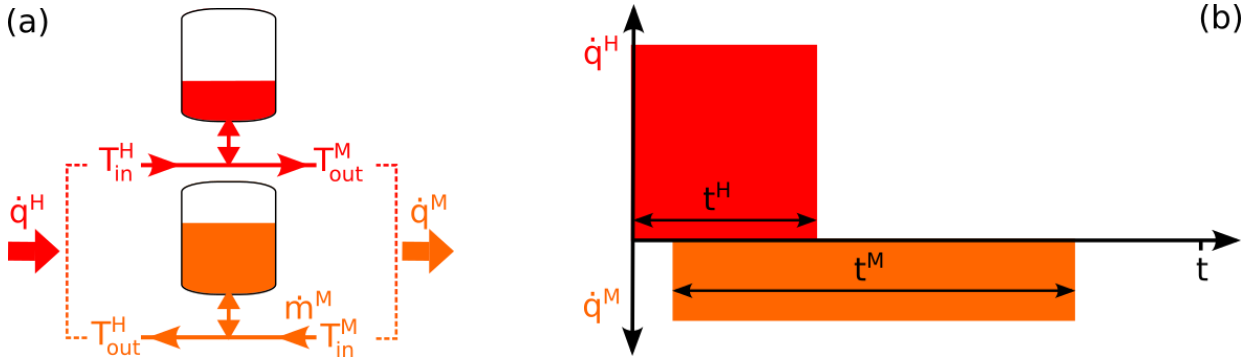

***Figure 1**. (a) 2-Tank TES system, (b) operation scenario*

Assuming a periodic stationary regime and no heat losses, energy and entropy balances related to the TES system write, on a period t:

$$\Delta U = \int_{t^H} \dot{m}^H \left(h^H_{in} - h^H_{out}\right) dt + \int_{t^M} \dot{m}^M \left(h^M_{in} - h^M_{out}\right) dt = 0 \tag{4}$$

$$\Delta S = \int_{t^H} \dot{m}^H \left(s^H_{in} - s^H_{out}\right) dt + \int_{t^M} \dot{m}^M \left(s^M_{in} - s^M_{out}\right) dt + \int_{t} \dot{\sigma}_{irr}\, dt = 0 \tag{5}$$

Posing

$$\dot{q}^H = \frac{1}{t^H} \int_{t^H} \dot{m}^H \left(h^H_{in} - h^H_{out}\right) dt \qquad \dot{q}^M = \int_{t^M} \dot{m}^M \left(h^M_{in} - h^M_{out}\right) dt \tag{6}$$

$$\tilde{T}^H = \frac{\int_{t^H} \dot{m}^H \left(h^H_{in} - h^H_{out}\right) dt}{\int_{t^H} \dot{m}^H \left(s^H_{in} - s^H_{out}\right) dt} \qquad \tilde{T}^M = \frac{\int_{t^M} \dot{m}^M \left(h^M_{in} - h^M_{out}\right) dt}{\int_{t^M} \dot{m}^M \left(s^M_{in} - s^M_{out}\right) dt} \tag{7}$$

Eqs. (3) and (4) simplify in:

$$\dot{q}^H t^H - \dot{q}^M t^M = 0 \tag{8}$$

$$\frac{\dot{q}^H t^H}{\tilde{T}^H} - \frac{\dot{q}^M t^M}{\tilde{T}^M} = -\int_{t} \dot{\sigma}_{irr}\, dt \leq 0 \tag{9}$$

Energy conservation (Eq. (8)) permits to express the 2nd law inequality according to the equivalent temperatures $\tilde{T}^H$ and $\tilde{T}^M$:

$$\tilde{T}^M - \tilde{T}^H \leq 0 \tag{10}$$

2.3. Equivalent power plant

The equivalence models allow any heat transfer fluid that undergoes a temperature change to be replaced by a thermostat whose temperature corresponds to the equivalence temperatures defined above. As an example, **Figure 2** presents the flowsheet of a CSP plant with indirect storage and its related equivalent model. All heat exchangers are replaced by a conductance, and every heat transfer fluid inlet/outlet by a thermostat. The process can be divided in three loops:

In the high temperature (HT) loop, the solar thermal flux $\dot{q}^H$ is collected and transferred to the TES system. The medium temperature (MT) loop picks up the thermal flux $\dot{q}^M$ from the TES system and transfers it to the power block. The power block consumes $\dot{q}^M$, and converts it in power $\dot{w}$ and thermal flux $\dot{q}^L$. The low temperature (LT) loop cools the power block and transfers the thermal flux $\dot{q}^L$ to the air through the cooling tower.

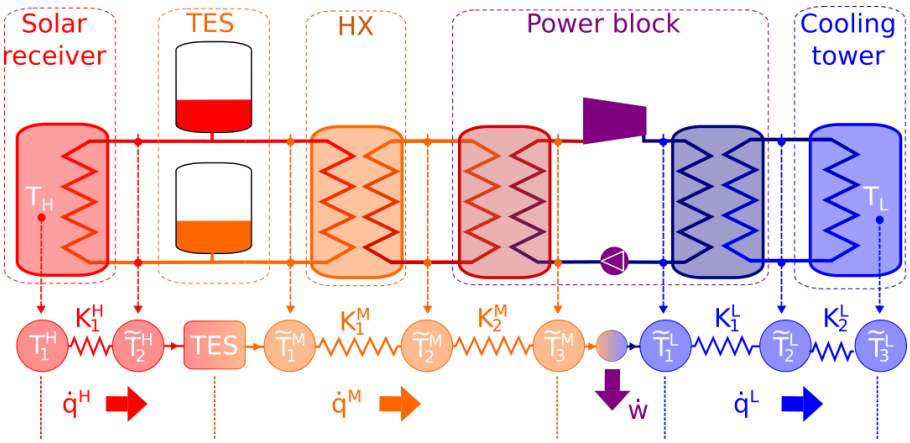

***Figure 2**. CSP plant with indirect storage. Schematic flowsheet and related equivalent system.*

2.3. Optimisation problem

To be as general as possible, the problem is defined for any number of heat exchangers in each loop. Thence, the power plant to be optimised includes (**Figure 3**):

- h heat exchangers in the HT loop,
- m heat exchangers in the MT loop,
- l heat exchangers in the LT loop.

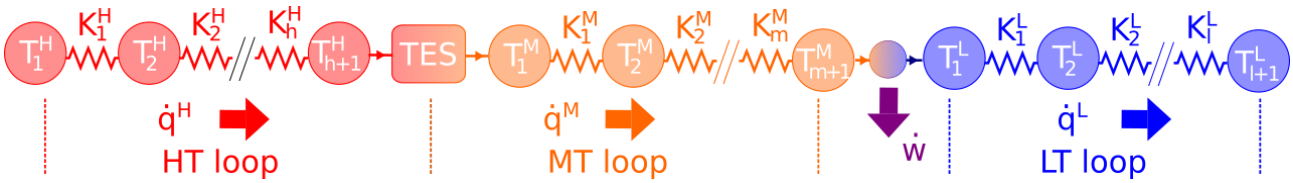

***Figure 3**. Equivalent system to be optimised.*

According to the operation scenario displayed **Figure 1b**, the mechanical energy produced per cycle is:

$$w = \dot{w}\, t^M \tag{11}$$

This quantity is maximised subjected to the following equality constraints:

1. conservation of energy for the TES, Eq. (8),
2. Newton's Law, Eq. (1), for each heat exchanger, in each loop,
3. conservation of energy for the power block, Eq. (2),
4. Equality of T_1^H and T_l^L with the temperature of the hot and cold sources,

$$T_1^H = \mathrm{T_H}, \qquad T_{l+1}^L = \mathrm{T_L} \tag{12}$$

Three inequality constraints also apply:

5. 2nd law related to the power block, Eq. (3),
6. 2nd law related to the TES system, Eq. (10),
7. Finite dimensions constraint: as each conductance must be finite, their sum is necessary also finite. Then, there exists a finite positive number K_Σ such as:

$$\sum_{i=1}^{h} K_i^H + \sum_{i=1}^{m} K_i^M + \sum_{i=1}^{l} K_i^L - K_\Sigma \leq 0 \tag{13}$$

The resolution of this optimisation problem is detailed in Appendix A. It involves $7 + 2 \cdot (h + m + l)$ optimisation variables (output power $\dot{w}$, heat fluxes $\dot{q}^H, \dot{q}^M$ and $\dot{q}^L$, $h + m + l$ conductances K_i^J, $h + m + l + 3$ temperatures T_i^J), and four optimisation parameters (durations t^H and t^M related to the operating scenario, and temperatures

of the heat source T_H and heat sink T_L). An optimal solution exists whatever the number of heat exchanger is. The main results are presented and discussed in the next section.

3. Results and discussion

The optimal solution is obtained for saturated inequality constraints (Eq. (A 31)-(A 33)).This shows logically that the TES system and the power block must be endoreversible, and that a higher K_Σ implies a higher output power. This last item appears clearly through the expression of the optimal power output (Eq. (A 66)):

$$\dot{w}^* = \frac{1}{\left(h\sqrt{t^M/t^H} + m + l\right)^2} K_\Sigma \left(\sqrt{T_H} - \sqrt{T_L}\right)^2 \tag{14}$$

which depends linearly on K_Σ. Equation (A 14) also shows how the number of heat exchangers affects the output power $\dot{w}^*$. As t^H and t^M are of same order of magnitude, the denominator represents approximatively the total number of heat exchangers $N_{HX} = h + m + l$. Thence, output power produced by the plant is approximately inversely proportional to N_{HX}. Impact of the TES can also be analysed. Increasing the ratio t^M/t^H, (i.e., increasing the storage capacity), reduces the capacity of the power block, but increases the mechanical energy provided during a cycle given by Eq. (11). **Figure 4** presents the evolution of output power $\dot{w}^*$ and mechanical energy $\dot{w}^*$ produced per day according to the production duration t^M and assuming t^H = 10 h (sunny hours in the case of CSP plant) for K_Σ = 10 MW/K, T_H = 30°C and T_H = 400°C. Three architectures are compared, all integrating an indirect cooling (cooling tower):

- Direct Steam Generation with direct storage, involving 3 HXs (h = 1, m = 0, l = 2)
- Indirect Steam Generation with direct storage, involving 3 HXs (h = 1, m = 1, l = 2)
- Indirect Steam Generation with indirect storage, involving 4 HXs (h = 1, m = 2, l = 2)

As t^H = 10h, t^M = 10 h correspond to no TES and t^M = 24 h to a continuous production implying a 14 h storage capacity.

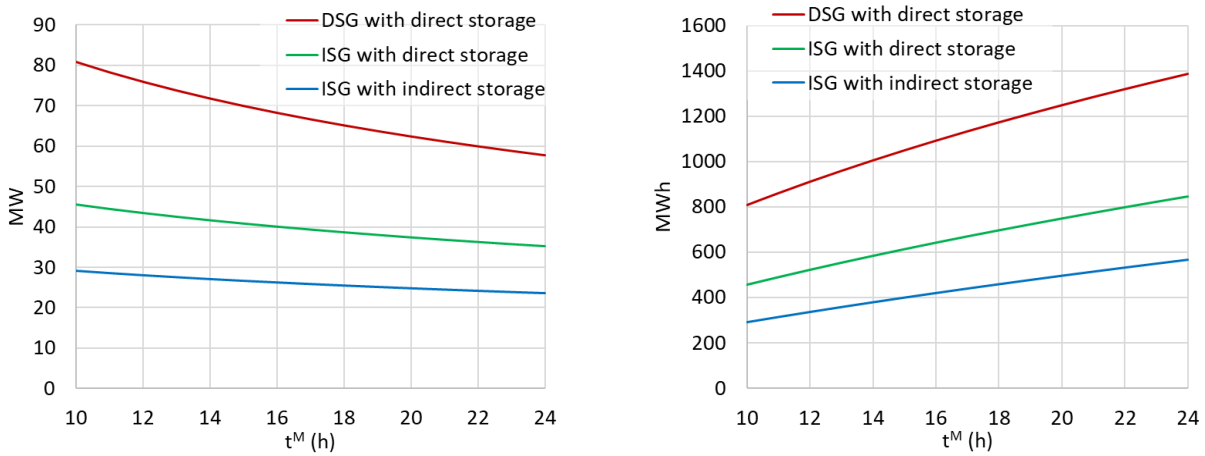

Figure 4. *Output power $\dot{w}^*$(a) and mechanical energy per day (b) according to the production duration.*

Influence of the number of HX is clearly displayed. For a constant K_Σ, which reflects the cost of the HXs, the output power or energy production evolves approximately with N_{HX}^{-2}, as mentioned above. Concerning the production duration, it decreases the power block capacity, but increases the daily production due to a longer production duration.

Another interesting result concerns the optimal conductances and driving forces. In each loop, all conductances (and consequently all driving forces because of Newton's Law) are equal. From Eqs. (A 43),(A 46) and (A 55) we have:

$$K^{L*} = K^{M*} \qquad \Delta T^{L*} = \sqrt{T_L/T_H}\ \Delta T^M \qquad \dot{q}^{L*} = \sqrt{T_L/T_H}\ \dot{q}^M \tag{15}$$

$$K^{H*} = \sqrt{t^M/t^H}\ K^* \qquad \Delta T^{H*} = \sqrt{t^M/t^H}\ \Delta T^M \qquad \dot{q}^{H*} = (t^M/t^H)\ \dot{q}^M \tag{16}$$

For the MT and LT loop downstream the TES, conductances are equal. Heat flux $\dot{q}^{L*}$ is lower $\dot{q}^{M*}$ because part of $\dot{q}^{M*}$ has been converted in power $\dot{w}^*$. Consequently, the driving force ΔT^{L*} is also lower than ΔT^{M*}.

For the HT loop, heat flux $\dot{q}^{H*}$ is higher then $\dot{q}^{M*}$, but here, the optimal solution shares equally this increase between the driving force ΔT^{K*} and the conductances K^{H*}

Finally, the energy efficiency of the plant can be deduced from (A 65) and (A 66):

$$\eta^* = \frac{\dot{w}^* t^M}{\dot{q}^{H*} t^H} = \frac{\dot{w}^*}{\dot{q}^{M*}} = 1 - \sqrt{\frac{T_L}{T_H}} \tag{17}$$

Thus, the optimal efficiency neither depends on the number of HXs, nor on the operating scenario, and is equal to the Curzon-Ahlborn efficiency. **Figure 5** compares the efficiency given by Eq.(17) with experimental efficiencies evaluated from available data sets covering many power plant architectures. The ORCs [17] correspond to the simpler structure: no TES ($t^M = t^H$), no MT loop ($m = 0$), direct or indirect cooling ($l = 1\ or\ 2$). Most of those displayed are laboratory prototypes. This could explain efficiencies sometimes much lower than η^*. For nuclear power plants [18], the hot source temperature (cladding maximum temperature) has been supposed to be 50°C higher than the reactor outlet temperature. Two architectures are presented, BWR ($h = 1$) and PWR ($h = 2$), the other parameters being similar ($t^M = t^H, m = 0, l = 1\ or\ 2$). Most of them reach or even overcome the optimal efficiency. Solar power plant [19] are also commercial plants, all including a TES, with various storage capacity ($2\ h\ < t_{storage}\ < 13\ h$), storage technology (m = 1 or 2), and involving a cooling tower (l = 2). Similarly to nuclear, the only hot temperature available in database was the solar field outlet temperature. Hot source temperatures (maximum temperature of the receiver wall) have been supposed to be 20°C (parabolic trough) or 50°C (tower) higher than the solar field outlet temperature. This figure clearly displays the fact that commercial plants, which have benefited for more than 40 years (solar) or 70 years (nuclear) of R&D fit quite well the η^* curve. That proves that Eq. (17) gives a good approximation of the efficiency of heat engines that have benefited from several decades of research and development. Therefore, we can reasonably assume that it also gives a good assessment of what the efficiency of emerging technologies will be in their future commercial form.

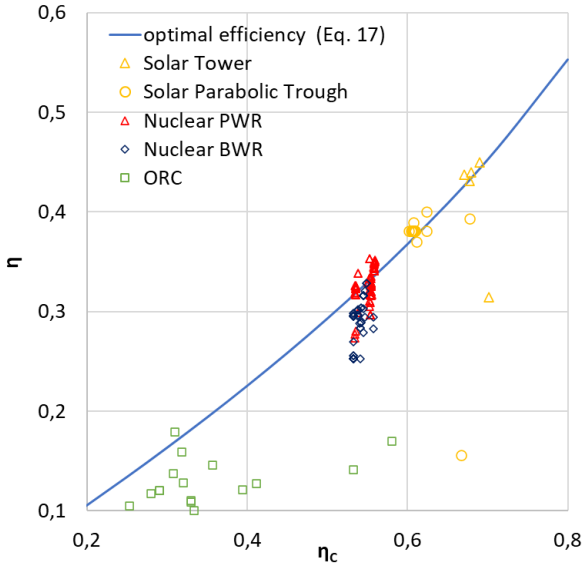

***Figure 5** : Energy efficiency of power plants from [17], [18], [19] data.*

4. Conclusion

This study aimed to extend FDT results to many power plant structures that may involve different numbers of heat exchangers and may operate with or without a TES. A general model was developed that determined the operating temperatures maximizing the power plant's output energy. A remarkable result is that the optimal efficiency is equal to the Curzon-Ahlborn efficiency, regardless the architecture of the plant and the operation scenario. However, the architecture of the plant impacts a lot the output power which varies approximatively with N_{HX}^{-2}. Concerning the operation scenario, increasing the storage capacity decreases the installed capacity of the power block but increases the daily energy output. Finally, the comparison of the actual efficiency of power plants shows that technologies that have benefited from several years of R&D achieve the Curzon Ahlborn efficiency. The latter could then be used to estimate the future performance of emerging technologies, such as combined cycles, or supercritical cycles. These technologies could take advantage of a higher temperature provided by generation IV nuclear reactors or future solar towers. Integrating these new technologies in the present analysis is one of the perspectives of this work.

Appendix A

The optimization problem is:

$\min(-\dot{w}\ t^M)$

s.t. $\dot{q}^H\ t^H - \dot{q}^M\ t^M = 0$ (A 1)

$K_i^J\left(T_i^J - T_{i+1}^J\right) - \dot{q}_i^J = 0\ , \forall\ J\ \in \{H,\ M, L\}, \forall\ i\ \in\ [1 \cdots n^J]$ (A 2)

$\dot{q}^H\ -\ \dot{q}^L -\ \dot{w} = 0$ (A 3)

$T_1^H = \mathrm{T_H}$ (A 4)

$T_{l+1}^L = \mathrm{T_L}$ (A 5)

$T_1^M - T_{h+1}^H \leq 0$ (A 6)

$\dot{q}^M/T_{m+1}^M - \dot{q}^L/T_1^L \leq 0$ (A 7)

$$\sum_{J=H,M,L}\left(\sum_{i=1}^{n^J} K_i^J\right) - K_\Sigma \leq 0 \quad \text{(A 8)}$$

The durations (t^H, t^M), the heat source temperatures ($\mathrm{T_H}$,$\mathrm{T_L}$) and the numbers of heat exchangers $n^H = h$, $n^M = m,\ n^L = l$) being taken as parameters, the Lagrangian function of this optimization problem writes:

$$\mathcal{L}\left(\dot{w}, \dot{q}^J, K_i^J, T_i^J, \lambda_i^J, \lambda_k, \mu_n\right) = \left\{\begin{array}{l} -\dot{w}\ t^M + \lambda_1(\dot{q}^H\ t^H -\ \dot{q}^M\ t^M) + \sum_{J=H,M,L}\left\{\sum_{i=1}^{n^J}\lambda_i^J\left[K_i^J\left(T_i^J - T_{i+1}^J\right) - \dot{q}^J\right]\right\} \\ +\lambda_2(\dot{q}^M -\ \dot{q}^L -\ \dot{w}) + \lambda_3(T_1^H - \mathrm{T_H}) + \lambda_4(T_{l+1}^L - \mathrm{T_L}) \\ +\mu_1(T_1^M - T_{h+1}^H) + \mu_2(\dot{q}^M/T_{m+1}^M - \dot{q}^L/T_1^L) + \mu_3\left[\sum_{J=H,M,L}\left(\sum_{i=1}^{n^J} K_i^J\right) - K_\Sigma\right] \end{array}\right\} \quad \text{(A 9)}$$

where $J\ \in \{H,\ M, L\}$, $i\ \in\ [1 \cdots n^J]$, $k\ \in\ [1 \cdots 5]$, $n \in\ [1 \cdots 2]$. The optimal conditions are:

$$\frac{\partial \mathcal{L}}{\partial \dot{w}} = -t^M -\ \lambda_2 = 0 \quad \text{(A 10)}$$

$$\frac{\partial \mathcal{L}}{\partial \dot{q}^H} = \lambda_1\ t^H - \sum_{i=1}^{h}\lambda_i^H = 0 \quad \text{(A 11)}$$

$$\frac{\partial \mathcal{L}}{\partial \dot{q}^M} = -\lambda_1\ t^M - \sum_{i=1}^{m}\lambda_i^M + \lambda_2 + \mu_2/T_{m+1}^M = 0 \quad \text{(A 12)}$$

$$\frac{\partial \mathcal{L}}{\partial \dot{q}^L} = -\sum_{i=1}^{l}\lambda_i^L - \lambda_2 - \mu_2/T_1^L = 0 \quad \text{(A 13)}$$

$$\frac{\partial \mathcal{L}}{\partial K_i^J} = \lambda_i^J\left(T_i^J - T_{i+1}^J\right) + \mu_3\ = 0, \forall\ J\ \in \{H, M, L\}, \forall\ i\ \in\ [2 \cdots n^J] \quad \text{(A 14)}$$

$$\frac{\partial \mathcal{L}}{\partial T_i^J} = \lambda_i^J K_i^J - \lambda_{i-1}^J K_{i-1}^J = 0, \qquad \forall\ J\ \in \{H, M, L\}, \qquad \forall\ i\ \in\ [2 \cdots n^J] \quad \text{(A 15)}$$

$$\frac{\partial \mathcal{L}}{\partial T_1^H} = \lambda_1^H K_1^H + \lambda_3 = 0 \quad \text{(A 16)}$$

$$\frac{\partial \mathcal{L}}{\partial T_{h+1}^{H}} = -\lambda_h^H K_h^H - \mu_1 = 0 \quad \text{(A 17)}$$

$$\frac{\partial \mathcal{L}}{\partial T_1^M} = \lambda_1^M K_1^M + \mu_1 = 0 \quad \text{(A 18)}$$

$$\frac{\partial \mathcal{L}}{\partial T_{m+1}^M} = -\lambda_m^M K_m^m - \mu_2 \, \dot{q}^M / (T_{m+1}^M)^2 = 0 \quad \text{(A 19)}$$

$$\frac{\partial \mathcal{L}}{\partial T_1^L} = \lambda_1^L K_1^L + \mu_2 \, \dot{q}^L / (T_1^L)^2 = 0 \quad \text{(A 20)}$$

$$\frac{\partial \mathcal{L}}{\partial T_{l+1}^L} = -\lambda_l^L K_l^L + \lambda_4 = 0 \quad \text{(A 21)}$$

$$\dot{q}^H \, t^H - \, \dot{q}^M \, t^M = 0 \quad \text{(A 22)}$$

$$K_i^J \left(T_i^J - T_{i+1}^J\right) - \dot{q}^J = 0, \qquad \forall \, J \in \{H, M, L\}, \qquad \forall \, i \in [1 \cdots n^J] \quad \text{(A 23)}$$

$$\dot{q}^H - \dot{q}^L - \dot{w} = 0 \quad \text{(A 24)}$$

$$T_1^H - \mathrm{T_H} = 0 \quad \text{(A 25)}$$

$$T_{l+1}^L - \mathrm{T_L} = 0 \quad \text{(A 26)}$$

$$\mu_1 (T_1^M - T_{h+1}^H) = 0, \qquad \mu_1 \geq 0, \quad \text{(A 27)}$$

$$\mu_2 (\dot{q}^M / T_{m+1}^M - \dot{q}^L / T_1^L) = 0, \qquad \mu_2 \geq 0 \quad \text{(A 28)}$$

$$\mu_3 \left(\sum_{J=H,M,L} \left(\sum_{i=1}^{n^J} K_i^J \right) - K_\Sigma \right) = 0, \qquad \mu_3 \geq 0 \quad \text{(A 29)}$$

We first demonstrate that μ_1, μ_2 and μ_3 cannot be null and then solve this system.

1. $\mu_3 = 0$

Equation (A 14) shows that all the λ_i^J should be zero, as $T_i^J - T_{i+1}^J = 0$ would imply, from (A 23), $\dot{q}^J = 0$ which is not acceptable. Therefore, $\mu_2 = 0$ from (A 19) or (A 20), and (A 13) implies that $\lambda_2 = 0$,which is forbidden from (A 10), the duration t^M being strictly positive:

$$\lambda_2 = -t^M \quad \text{(A 30)}$$

Hence, $\mu_3 \neq 0$

2. $\mu_1 = 0$

Equation (A 18) shows that λ_1^M should be zero as $K_1^M = 0$ would imply, , from (A 23), $\dot{q}^M = 0$, which is not acceptable. Therefore, Eq. (A 15) implies that all $\lambda_i^M = 0$ because $K_\mathrm{j}^M = 0$ would also implies $\dot{q}^M = 0$. Thence, $\mu_2 = 0$ from Eq. (A 19), which is not acceptable as seen above. Hence, $\mu_1 \neq 0$

3. $\mu_2 = 0$

Equations (A 19) shows that $\lambda_m^M = 0$ as $K_m^M = 0$ is not acceptable, because it would imply, from (A 23), $\dot{q}^M = 0$. Therefore, $\mu_2 = 0$ from (A 14), which is forbidden as seen above. Hence, $\mu_2 \neq 0$

4. $\mu_1 \neq 0$ and $\mu_2 \neq 0$ and $\mu_3 \neq 0$

Equations (A 28) and (A 29) then write:

$$T_1^M = T_{h+1}^H = \mathrm{T_{TES}}, \qquad \mu_1 \geq 0 \quad \text{(A 31)}$$

$$\frac{\dot{q}^M}{T_{m+1}^M} - \frac{\dot{q}^L}{T_1^L} = 0, \qquad \mu_2 > 0 \quad \text{(A 32)}$$

$$\sum_{i=1}^{h} K_i^H + \sum_{i=1}^{m} K_i^M + \sum_{i=1}^{l} K_i^L - K_\Sigma = 0, \quad \mu_3 > 0 \tag{A 33}$$

Equations (A 31) and (A 32) demonstrates that, quite logically:

- the optimal TES system operates reversibly,
- the optimal power block is an endoreversible engine.

Equations (A 14) and (A 23) imply:

$$\lambda_i^J = -\frac{\mu_3}{\left(T_i^J - T_{i+1}^J\right)} = -\mu_3 \frac{K_i^J}{\dot{q}^J}, \qquad \forall\, J \in \{H, M, L\}, \qquad \forall\, i \in [2 \cdots n^J] \tag{A 34}$$

Replacing λ_i^J in Eq. (A 15) gives:

$$-\frac{\mu_3}{\dot{q}^J}\left[\left(K_i^J\right)^2 - \left(K_{i-1}^J\right)^2\right] = 0, \qquad \forall\, J \in \{H, M, L\}, \qquad \forall\, i \in [2 \cdots n^J] \tag{A 35}$$

showing that, in each loop (i.e., HT, MT, or LT loops), all the conductances are equal.

$$K_i^H = K^H, \quad K_i^M = K^M, \quad K_i^L = K^M, \qquad \forall\, i \tag{A 36}$$

That also implies, from Eq. (A 34):

$$\lambda_i^H = -\mu_3 \frac{K^H}{\dot{q}^H} = \lambda^H, \qquad \lambda_i^M = -\mu_3 \frac{K^M}{\dot{q}^M} = \lambda^M, \qquad \lambda_i^L = -\mu_3 \frac{K^L}{\dot{q}^L} = \lambda^L, \qquad \forall\, i \tag{A 37}$$

$$T_i^H - T_{i+1}^H = \frac{\dot{q}^H}{K^H} = \Delta T^H, \quad T_i^M - T_{i+1}^M = \frac{\dot{q}^M}{K^M} = \Delta T^M, \quad T_i^L - T_{i+1}^L = \frac{\dot{q}^L}{K^L} = \Delta T^L, \quad \forall\, i \tag{A 38}$$

Introducing the expressions of λ_i^J in Eqs.(A 11) (A 16),(A 17),(A 18) and (A 21) gives:

$$\lambda_1 = -\mu_3 \frac{h\, K^H}{\dot{q}^H\, t^H} \tag{A 39}$$

$$\lambda_3 = \mu_3 \frac{(K^H)^2}{\dot{q}^H} \tag{A 40}$$

$$\mu_1 = \mu_3 \frac{(K^H)^2}{\dot{q}^H} = \mu_3 \frac{(K^M)^2}{\dot{q}^M} \tag{A 41}$$

$$\lambda_4 = -\mu_3 \frac{(K^L)^2}{\dot{q}^L} \tag{A 42}$$

Equations (A 22), (A 41) and (A 38) imply:

$$\dot{q}^H = \tau\, \dot{q}^M, \qquad K^H = \sqrt{\tau}\, K^M, \qquad \Delta T^H = \sqrt{\tau}\, \Delta T^M \tag{A 43}$$

with $\tau = t^M / t^H$

Expressing μ_2 from Eqs. (A 19) and (A 20), and using (A 36) and (A 37) gives:

$$\mu_2 = \mu_3 (K^M)^2 \left(\frac{T_{m+1}^M}{\dot{q}^M}\right)^2 = \mu_3 (K^L)^2 \left(\frac{T_1^L}{\dot{q}^L}\right)^2 \tag{A 44}$$

showing that, using (A 32):

$$K^M = K^L = K^* \tag{A 45}$$

Introducing Eqs. (A 43) and (A 45) in Eq. (A 33) gives the optimal values of the conductance K^*:

$$\mathrm{h} \cdot \sqrt{\tau}\, \mathrm{K}^* + \mathrm{m} \cdot \mathrm{K}^* + \mathrm{l} \cdot \mathrm{K}^* = K_\Sigma \implies \mathrm{K}^* = \frac{K_\Sigma}{\mathrm{h} \cdot \sqrt{\tau} + m + l} \tag{A 46}$$

Introducing the expression of λ_1(A 39), λ_2 (A 30), μ_2(A 44) and λ_i^J(A 37) in Equations (A 12) and (A 13) gives:

$$\mu_3 \left[h \frac{K^H}{\dot{q}^H} \frac{t^M}{t^H} + \mathrm{m} \ \frac{K^M}{\dot{q}^M} + T_{m+1}^M \left(\frac{K^M}{\dot{q}^M} \right)^2 \right] = t^M \quad \text{(A 47)}$$

$$\mu_3 \left[-l \ \frac{K^L}{\dot{q}^L} + T_1^L \left(\frac{K^L}{\dot{q}^L} \right)^2 \right] = t^M \quad \text{(A 48)}$$

Using (A 38) and (A 43), Equations (A 47) and (A 48) write:

$$\frac{\mu_3}{\Delta T^M} \left[h\sqrt{\tau} \ + \mathrm{m} + \frac{T_{m+1}^M}{\Delta T^M} \right] = t^M \quad \text{(A 49)}$$

$$\frac{\mu_3}{\Delta T^L} \left[-l \ + \frac{T_1^L}{\Delta T^L} \right] = t^M \quad \text{(A 50)}$$

Thence,

$$\mu_3 = \frac{t^M (\Delta T^M)^2}{\left(h\sqrt{\tau} \ + m \right) \Delta T^M + T_{m+1}^M} = \frac{t^M (\Delta T^L)^2}{-l \, \Delta T^L + T_1^L} \quad \text{(A 51)}$$

Combining (A 43), (A 25) and (A 31) gives:

$$\left(h\sqrt{\tau} \ + m \right) \Delta T^M = h \, \Delta T^H + \ m \, \Delta T^M = T_1^H - T_{h+1}^H + T_1^M - T_{m+1}^M = T_H - T_{m+1}^M \quad \text{(A 52)}$$

In a similar way, we have, using (A 26)

$$l \, \Delta T^L = T_1^L - T_{l+1}^L = T_1^L - T_L \quad \text{(A 53)}$$

Thence, Eq. (A 51) simplifies in:

$$\mu_3 = \frac{t^M (\Delta T^M)^2}{T_H} = \frac{t^M (\Delta T^L)^2}{T_L} \quad \text{(A 54)}$$

showing that:

$$\Delta T^L = \sqrt{\frac{T_L}{T_H}} \, \Delta T^M \, . \quad \text{(A 55)}$$

Combining (A 38), (A 44) and (A 55) gives:

$$\mu_2 = \mu_3 \left(\frac{T_{m+1}^M}{\Delta T^M} \right)^2 = \mu_3 \left(\frac{T_1^L}{\Delta T^L} \right)^2 \implies T_1^L = \frac{\Delta T^L}{\Delta T^M} \, T_{m+1}^M = \sqrt{\frac{T_L}{T_H}} \, T_{m+1}^M \quad \text{(A 56)}$$

Introducing (A 55) and (A 56) in (A 53) gives

$$l \sqrt{\frac{T_L}{T_H}} \, \Delta T^M = \sqrt{\frac{T_L}{T_H}} \, T_{m+1}^M - T_L \implies T_{m+1}^M = \sqrt{T_H T_L} + l \ \Delta T^M \quad \text{(A 57)}$$

Thence, (A 52) writes :

$$\left(h\sqrt{\tau} \ + m \right) \Delta T^M = T_H - \sqrt{T_H T_L} - l \ \Delta T^M \quad \text{(A 58)}$$

which gives the optimal expressions of ΔT_M^*:

$$\Delta T^{M*} = \frac{T_H - \sqrt{T_H T_L}}{h\sqrt{\tau} \ + m + l} \quad \text{(A 59)}$$

ΔT^{H*} and ΔT^{L*} are deduced respectively from (A 43) and (A 55):

$$\Delta T^{H*} = \sqrt{\tau} \frac{T_H - \sqrt{T_H T_L}}{h\sqrt{\tau} \ + m + l}, \qquad \Delta T^{L*} = \frac{\sqrt{T_H T_L} - T_L}{h\sqrt{\tau} \ + m + l} \quad \text{(A 60)}$$

All the optimization variables can be now deduced.

Conductances

Optimal conductances are given by Eqs (A 43), (A 45) and (A 46):

$$K_i^{L*} = K_i^{M*} = K^* = \frac{K_\Sigma}{\mathrm{h}\cdot\sqrt{\tau}+m+l}, \qquad K_i^{H*} = \sqrt{\tau}\,K^* = \frac{\sqrt{\tau}\,K_\Sigma}{\mathrm{h}\cdot\sqrt{\tau}+m+l} \tag{A 61}$$

Temperatures

The optimal temperature bounding the power block write, using (A 56) and (A 57):

$$T_{m+1}^{M*} = \frac{l\,T_H + \left(h\sqrt{\tau}\,+m\right)\sqrt{T_H T_L}}{h\sqrt{\tau}\,+m+l}, \qquad T_1^{L*} = \frac{l\,\sqrt{T_H T_L} + \left(h\sqrt{\tau}\,+m\right)T_L}{h\sqrt{\tau}\,+m+l}, \tag{A 62}$$

The optimal temperature of the TES ($T_{TES} = T_{h+1}^{H} = T_1^{M}$) can be deduced from (A 59) and (A 62) reminding that $m\,\Delta T^M = T_1^M - T_{m+1}^M$:

$$T_{TES}^* = \frac{(l+m)\,T_H + h\sqrt{\tau}\,\sqrt{T_H T_L}}{h\sqrt{\tau}\,+m+l} \tag{A 63}$$

General expressions for the temperatures are:

$$\begin{aligned} T_{i+1}^{H*} &= T_H - i\;\Delta T^{H*}, & i &= 0..h \\ T_{i+1}^{M*} &= T_{TES} - i\,\Delta T^{M*} & i &= 0..m \\ T_{i+1}^{L*} &= T_L + (l-i)\,\Delta T^{L*}, & i &= 0..l \end{aligned} \tag{A 64}$$

Heat flows and mechanical power

The heat flows are obtained using (A 43), (A 45),(A 46),(A 59) and (A 60):

$$\dot{q}^{H*} = \tau\,K_\Sigma\frac{T_H - \sqrt{T_H T_L}}{\left(h\sqrt{\tau}\,+m+l\right)^2}, \quad \dot{q}^{M*} = K_\Sigma\frac{T_H - \sqrt{T_H T_L}}{\left(h\sqrt{\tau}\,+m+l\right)^2}, \qquad \dot{q}^{L*} = K^*\frac{\sqrt{T_H T_L} - T_L}{\left(h\sqrt{\tau}\,+m+l\right)^2} \tag{A 65}$$

Mechanical power is obtained from (A 24). Using (A 65), we get:

$$\dot{w}^* = K_\Sigma\frac{\left(\sqrt{T_H} - \sqrt{T_L}\right)^2}{\left(h\sqrt{\tau}\,+m+l\right)^2} \tag{A 66}$$

Lagrange multipliers

Combining Eqs. (A 41), (A 54) and (A 56) gives:

$$\mu_1^* = t^M\frac{\dot{q}^{M*}}{T_H} > 0 \qquad \mu_2^* = \frac{t^M}{T_H}(T_{m+1}^{M*})^2 > 0 \qquad \mu_3^* = \frac{t^M}{T_H}(\Delta T^{M*})^2 > 0 \tag{A 67}$$

From Eqs. (A 37) to (A 42), combined with (A 54),(A 55) and (A 61) , we get

$$\begin{aligned} &\lambda_1^* = -\,h\,\frac{\Delta T^{H*}}{T_H}, \qquad \lambda_2^* = -t^M, \qquad \lambda_3^* = t^M\frac{\dot{q}^{M*}}{T_H}, \qquad \lambda_4^* = -t^M\frac{\dot{q}^{L*}}{T_L} \\ &\lambda_i^{H*} = -\,t^H\frac{\Delta T^{H*}}{T_H}, \qquad \lambda_i^{M*} = t^M\frac{\Delta T^{M*}}{T_H}, \quad \lambda_i^{L*} = -\,t^M\frac{\Delta T^{L*}}{T_L}, \qquad \forall\, i \end{aligned} \tag{A 68}$$

Nomenclature

h specific enthalpy, J/kg

K conductance, W/K

$\dot{m}$ mass flow rate, kg/s

$\dot{q}$ thermal flux, W

s specific entropy, J/(kg.K)

T temperature, °C

U Internal energy , J

S Entropy, J/K

$\dot{w}$ output power, W

Greek symbols

λ Lagrange multiplier (equality constraint)

Δ difference

η efficiency

μ Lagrange multiplier (inequality constraint)

$\dot{\sigma}$ internal entropy generation, W/K

τ operating durations ratio, $= t^M/t^H$

Subscripts and superscripts

H high temperature

h HX number in the high temperature loop

L low temperature

l HX number in the low temperature loop

M medium temperature

m HX number in the medium temperature loop

References

[1] S. Carnot, *Réflexions sur la puissance motrice du feu et sur les machines propres à développer cette puissance*. Bachelier Libraire, 1824.

[2] P. Chambadal, *Les centrales nucléaires*, Paris : A. Colin, 1957. in Armand Colin, 321. Section physique.

[3] I. I. Novikov, 'The efficiency of atomic power stations (a review)', *Journal of Nuclear Energy (1954)*, vol. 7, no. 1–2, pp. 125–128, Aug. 1958, doi: 10.1016/0891-3919(58)90244-4.

[4] F. L. Curzon and B. Ahlborn, 'Efficiency of a Carnot engine at maximum power output', *American Journal of Physics*, vol. 43, no. 1, pp. 22–24, Jan. 1975, doi: 10.1119/1.10023.

[5] A. D. Vos, 'Reflections on the power delivered by endoreversible engines', *J. Phys. D: Appl. Phys.*, vol. 20, no. 2, p. 232, Feb. 1987, doi: 10.1088/0022-3727/20/2/014.

[6] A. Bejan, 'Theory of heat transfer-irreversible power plants', *International Journal of Heat and Mass Transfer*, vol. 31, no. 6, pp. 1211–1219, Jun. 1988, doi: 10.1016/0017-9310(88)90064-6.

[7] A. Bejan, 'Entropy generation minimization: The new thermodynamics of finite-size devices and finite-time processes', *Journal of Applied Physics*, vol. 79, no. 3, pp. 1191–1218, Feb. 1996, doi: 10.1063/1.362674.

[8] M. Feidt, *Finite Physical Dimensions Optimal Thermodynamics 2 : Complex Systems*. Elsevier Science, 2018.

[9] C. H. Blanchard, 'Coefficient of performance for finite speed heat pump', *Journal of Applied Physics*, vol. 51, no. 5, p. 2471, 1980, doi: 10.1063/1.328020.

[10] M. Schaller, K. H. Hoffmann, R. Rivero, B. Andresen, and P. Salamon, 'The Influence of Heat Transfer Irreversibilities on the Optimal Performance of Diabatic Distillation Columns', *Journal of Non-Equilibrium Thermodynamics*, vol. 27, no. 3, Jan. 2002, doi: 10.1515/JNETDY.2002.015.

[11] M. J. Ondrechen, B. Andresen, and R. S. Berry, 'Thermodynamics in finite time: Processes with temperature-dependent chemical reactions', *The Journal of Chemical Physics*, vol. 73, no. 11, pp. 5838–5843, Dec. 1980, doi: 10.1063/1.440026.

[12] J. M. Gordon and Y. Zarmi, 'Wind energy as a solar-driven heat engine: A thermodynamic approach', *American Journal of Physics*, vol. 57, no. 11, pp. 995–998, Nov. 1989, doi: 10.1119/1.15783.

[13] D. Vos and A, 'Endoreversible thermodynamics of solar energy conversion', Jan. 1992, Accessed: Mar. 21, 2023. [Online]. Available: https://www.osti.gov/biblio/6010938

[14] F. Meunier, P. Neveu, and J. Castaing-Lasvignottes, 'Equivalent Carnot cycles for sorption refrigeration: Cycles de Carnot équivalents pour la production de froid par sorption', *International journal of refrigeration*, vol. 21, no. 6, pp. 472–489, 1998.

[15] J. Castaing-Lasvignottes and P. Neveu, 'Equivalent Carnot cycle concept applied to a thermochemical solid/gas resorption system', *Applied thermal engineering*, vol. 18, no. 9–10, pp. 745–754, 1998.

[16] P. Neveu, F. Ayachi, C. Leray, and Y. Azoumah, 'Optimal integration of rankine cycles in concentrated sol power plant', presented at the ECOS 2015 - 28th International Conference on Efficiency, Cost, Optimization, Simulation and Environmental Impact of Energy Systems, 2015.

[17] A. Landelle, N. Tauveron, P. Haberschill, R. Revellin, and S. Colasson, 'Organic Rankine cycle design and performance comparison based on experimental database', *Applied Energy*, vol. 204, pp. 1172–1187, Oct. 2017, doi: 10.1016/j.apenergy.2017.04.012.

[18] I. A. E. Agency, 'Operating Experience with Nuclear Power Stations in Member States', International Atomic Energy Agency, Text, 2020. Accessed: Mar. 30, 2023. [Online]. Available: https://www.iaea.org/publications/14782/operating-experience-with-nuclear-power-stations-in-member-states

[19] J. Thonig and R. Lilliestam, 'CSP.guru 2022-07-01 (2022-07-01) [Data set]. Zenodo.https://doi.org/10.5281/zenodo.7112761'. 2022.